

Electronic Supplementary Information

Properties of in situ generated gold nanoparticles in the cellular context

*Daniela Drescher, Heike Traub, Tina Büchner, Norbert Jakubowski, and Janina Kneipp**

Additional Data and Information

| | |
|---|---|
| Enlarged LA-ICP-MS maps of gold intensity in fibroblast cells | 2 |
| Quantification of the number of gold nanoparticles in cells | 3 |
| Transmission electron microscopy of tetrachloroauric acid in fibroblasts | 4 |
| Physicochemical properties of tetrachloroauric acid in cell media | 4 |
| Influence of H _{AuCl} ₄ concentration and incubation time on the SERS information | 5 |
| Assignment of the most frequently observed SERS signals | 7 |
| Laser parameters in the LA-ICP-MS experiments | 8 |

Enlarged LA-ICP-MS maps of gold intensity distribution in fibroblasts

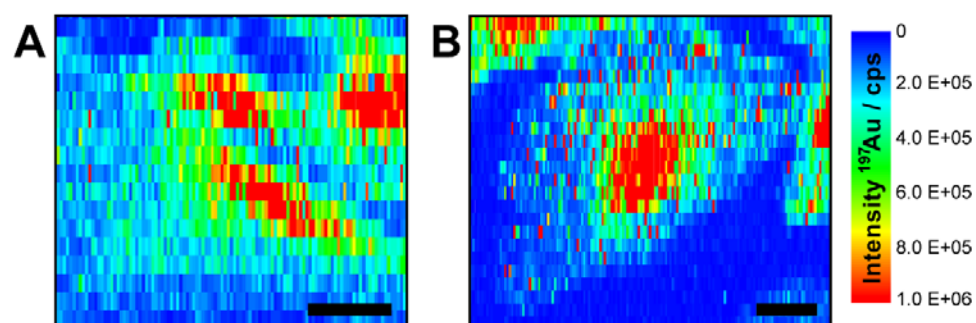


Figure S1. Details from Figure 1 in the manuscript. Intensity distribution of $^{197}\text{Au}^+$ in single fibroblast cells after 24h-exposure to 1 mM tetrachloroauric acid (**A**) in PBS and (**B**) in DMEM with 10 % FCS determined by LA-ICP-MS. Single pixels of high $^{197}\text{Au}^+$ intensity are observed in the cytoplasm of the fibroblast cells for incubation of HAuCl_4 in DMEM with 10 % FCS (**B**), which do not occur upon incubation in PBS (**A**). Parameters: laser spot size $4\ \mu\text{m}$, line distance $6\ \mu\text{m}$, scan speed $5\ \mu\text{m/s}$, frequency 10 Hz, pixel size $6 \times 1\ \mu\text{m}$, fluence $0.7\ \text{J/cm}^2$.

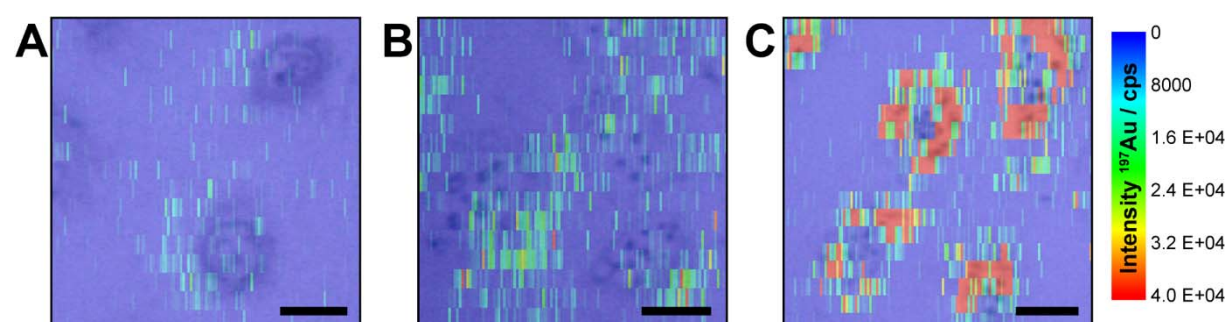


Figure S2. Details from Figure 2 in the manuscript. Intensity distribution of $^{197}\text{Au}^+$ in individual 3T3 fibroblasts after gold nanoparticle incubation for (**A**) 1 hour, (**B**) 3 hours and (**C**) 24 hours measured by LA-ICP-MS and the corresponding bright field images. With increasing incubation time, gold nanoparticles accumulate in the perinuclear region, while only low $^{197}\text{Au}^+$ signal intensities are determined in the nucleus region. These could originate from particles above and below the cell nucleus and maybe a few particles that entered the nucleus. Parameters: laser spot size $4\ \mu\text{m}$, line distance $6\ \mu\text{m}$, scan speed $5\ \mu\text{m/s}$, frequency 10 Hz, pixel size $6 \times 1\ \mu\text{m}$, fluence $0.7\ \text{J/cm}^2$.

Quantification of the number of gold nanoparticles in cells

LA-ICP-MS data can also be used to determine the relative amount of nanoparticles at the single-cell-level and to compare different incubation conditions (Figure S3, light gray bars). The 2D LA-ICP-MS intensity maps were used to calculate the integrated $^{197}\text{Au}^+$ intensity of each single cell by ImageJ software. To compare the relative number of particles with absolute values, additional ICP-MS experiments were conducted after digestion of the cells (Figure S3, dark gray bars). The nanoparticle-incubated fibroblast cells were digested with aqua regia and the cell digests were analyzed using an iCAP Qc ICP-MS (Thermo Fisher Scientific, Germany, for operating parameters see Table S4) to determine the gold concentration. Details about the digestion and the ICP-MS analysis were described previously by Büchner *et al.*¹ The results (Figure S3) indicate a similar relative particle number for both methods, confirming the validity of the LA-ICP-MS experiments for the quantification of nanoparticles at the single-cell-level. The number of particles per cell increases with increasing incubation time from 13,000 after 1 hour to 227,000 nanoparticles after 24 hours. These values are based on the assumption of spherical particle morphology and a diameter of 14 nm (determined by TEM) and include both the internalized particles and the adsorbed particles on the cell membrane that have not been removed by washing with PBS. The number of particles in an individual cell differs very much, as reflected by the standard deviation bars of the LA-ICP-MS results (Figure S3, light gray bars). This can be attributed to differences in the size and morphology of the individual cells and their uptake behavior.

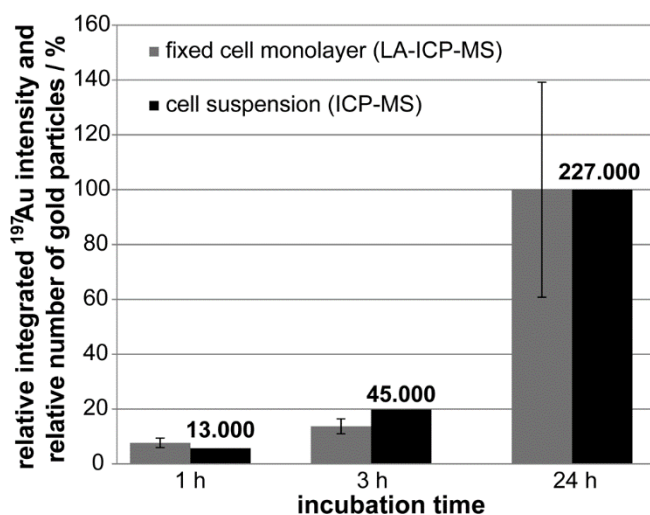


Figure S3. Relative integrated $^{197}\text{Au}^+$ intensity of single fibroblast cells based on the LA-ICP-MS maps shown in Figure 2A-C (bright gray bars) and the relative number of gold nanoparticles per cell determined by ICP-MS analysis after digestion of a cell pellet (dark gray bars). Fibroblast cells were incubated with gold nanoparticles for 1, 3 and 24 hours, respectively. The integrated intensity (bright gray bars) is given as mean value of 10-15 fibroblast cells.

Transmission electron microscopy of tetrachloroauric acid in fibroblasts

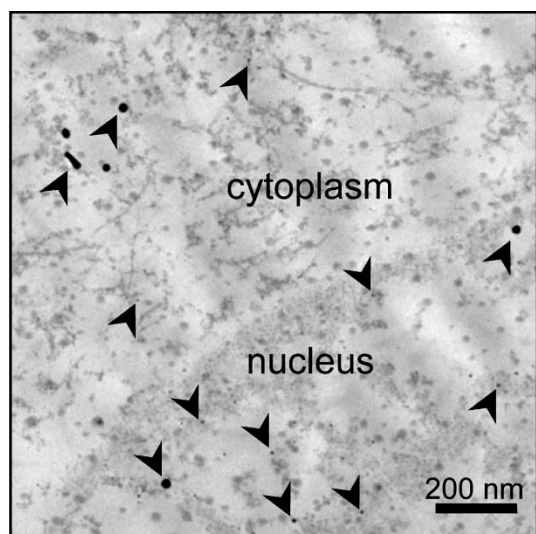


Figure S4. Transmission electron micrographs of 3T3 fibroblast cells after incubation with 1 mM tetrachloroauric acid in PBS buffer for 24 hours (detail from Figure 4A). Arrows point at the *in situ* formed nanoparticles also in the cell nucleus.

Physicochemical properties of tetrachloroauric acid in cell media

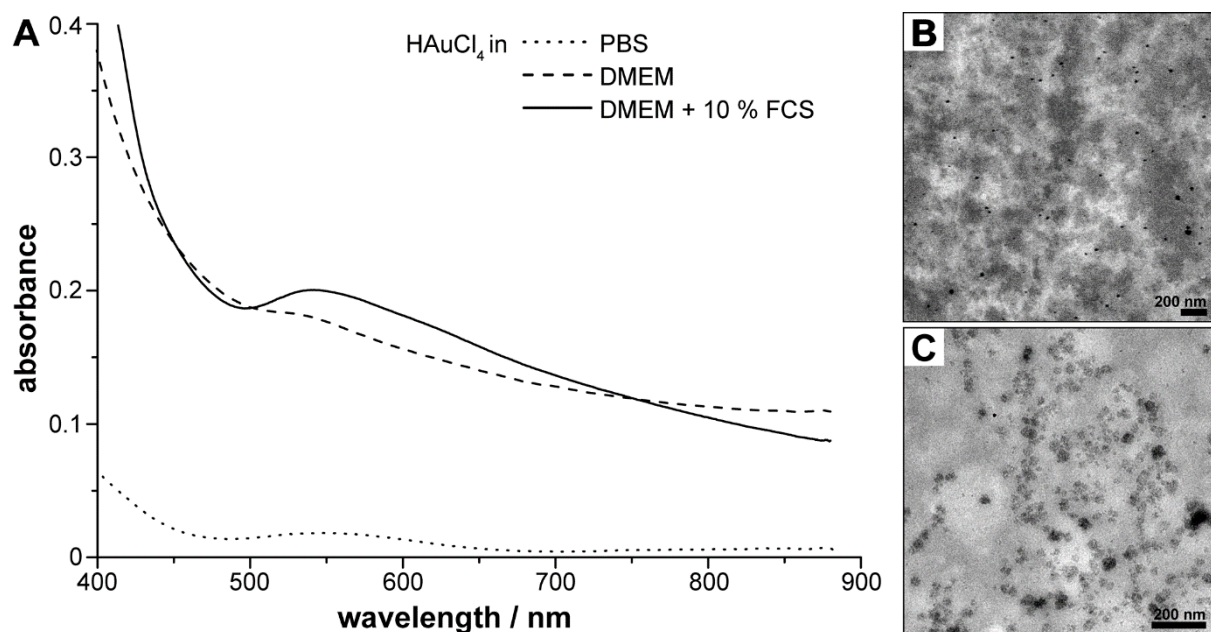


Figure S5. (A) UV-vis absorbance spectra of tetrachloroauric acid in PBS, DMEM, DMEM and 10 % fetal calf serum (FCS). TEM images were obtained after incubation of HAuCl_4 with (B) DMEM and (C) DMEM with 10 % FCS.

Influence of H_{AuCl}₄ concentration and incubation time on the SERS information

To investigate the influence of H_{AuCl}₄ concentration and incubation time on the intracellular formation of gold nanostructures, fibroblast cells were exposed to 0.25 mM and 0.1 mM H_{AuCl}₄ in PBS for 24 hours and 48 hours. Representative SERS spectra of these experiments are shown in Figure S6. Some vibrational modes such as the ring breathing vibration of tryptophan at 760 cm⁻¹, C-H deformation vibration at 1030 cm⁻¹ and the amide III band and CH₂/CH₃ deformation vibration at 1265 cm⁻¹ (for band assignments see Table S1) are only detected for the incubation of 0.25 mM H_{AuCl}₄ (Figure S6c, d). When a concentration of 0.1 mM H_{AuCl}₄ is used, signals at 565 cm⁻¹ (skeletal vibrations) and 1525 cm⁻¹ (amide II) are observed, which do not occur at higher concentrations (Figure S6a, b). Most of the bands in the SERS spectra (see also Table S1), especially the ring breathing vibration of tyrosine at 390 cm⁻¹, the S-S stretching vibration around 450 cm⁻¹ and the C-S stretching vibration of cysteine and tyrosine side chain at 665 / 690 cm⁻¹ occur arbitrarily and are thus independent of the H_{AuCl}₄ concentration (0.25 mM and 0.1 mM) and incubation time (24 h and 48 h). The continuance of the spectral fingerprint suggests a stable interaction of the nanostructures formed *in situ* with the molecules of the cell over the whole time of the experiment. SERS spectra obtained by incubation of lower H_{AuCl}₄ concentrations (Figure S6) show a greater accordance of the spectral fingerprint with that of nanoparticle-incubated cells (Figure 6F, G). When shorter incubation times (6 hours) and lower concentrations of H_{AuCl}₄ (0.01 mM) are used for the intracellular formation of nanoparticles in PBS, no SERS signals are observed. For the incubation with H_{AuCl}₄ in DMEM with 10 % FCS, SERS spectra were neither obtained for the non-toxic concentration of 0.1 mM H_{AuCl}₄, nor for the concentration of 0.25 mM, the latter shown to be toxic after 24 hours of incubation (Figure 5A).

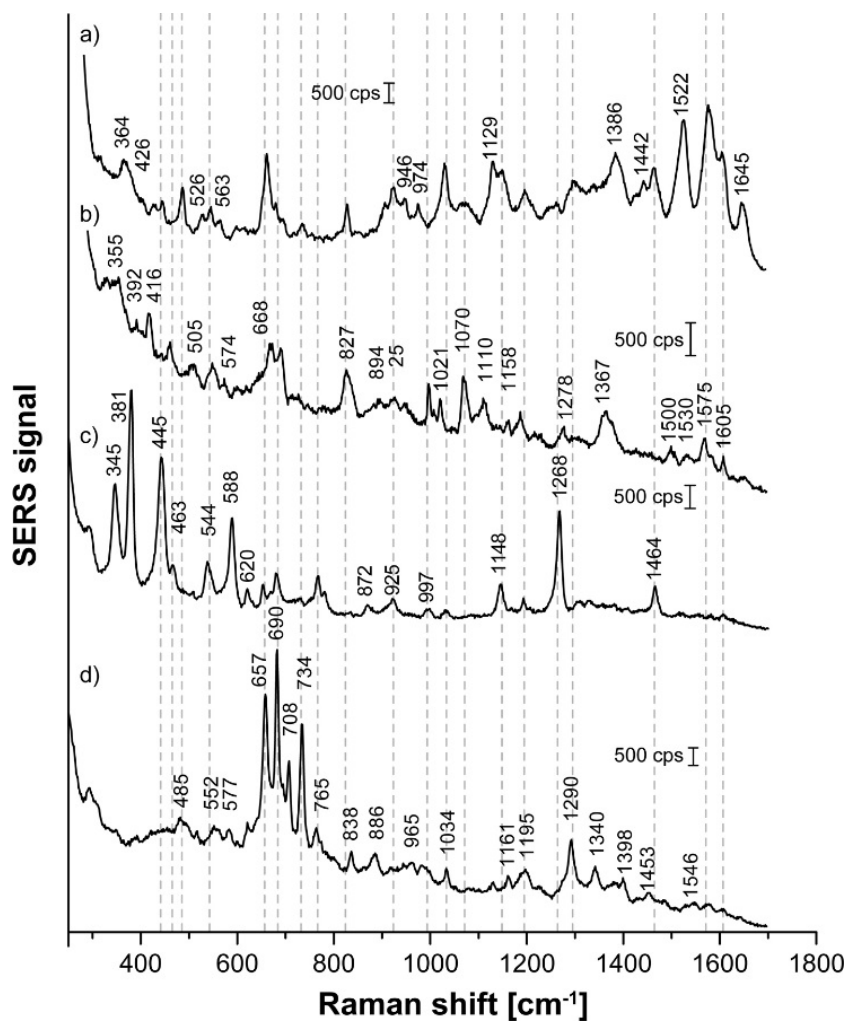


Figure S6. SERS spectra of 3T3 fibroblast cells exposed to different concentrations of tetrachloroauric acid in PBS buffer. Cells were incubated with 0.1 mM (**a, b**) and 0.25 mM (**c, d**) HAuCl₄ for 24 hours (**a, c**) and 48 hours (**b, d**). Representative spectra of individual cells are shown. Excitation wavelength: 785 nm, accumulation time: 1 s, intensity: $1.9 \times 10^5 \text{ W cm}^{-2}$.

Table S1. Assignment of the most frequently observed SERS signals in 3T3 fibroblast cells exposed to 1 mM tetrachloroauric acid in PBS buffer and in DMEM and to 0.1 nM gold nanoparticles sized 13 nm for 24 hours (see example spectra in Figure 6), respectively, to proteins, lipids, and nucleic acids. SERS signals marked grey highlight the bars in Figure 7. Abbreviations: Tyr, tyrosine; Cys, cysteine; Trp, tryptophan; Phe, phenylalanine; Thr, threonine; G, guanine; A, adenine; C, cytosine; sym, symmetric.²⁻⁹

| SERS signals of fibroblasts | | | Tentative band assignments | |
|-----------------------------|----------------------------|--------------------|---|---|
| HAuCl ₄ in PBS | HAuCl ₄ in DMEM | Gold nanoparticles | Proteins and lipids | Nucleic acids |
| 415 | 425 | | ring breath of Tyr | |
| | | 445 | S-S stretch of proteins | |
| | 490 | 500 | S-S stretch of proteins | |
| 545 | 545 | | skeletal deform and S-S stretch of proteins | G? |
| | | 565 | skeletal deform | |
| 590 | | | | |
| 620 | 617 | 635 | COO ⁻ wag, C-C twisting | |
| 655 | | 645 | C-S stretch of Cys, Tyr side chain | |
| 680 | 680 | 680 | C-S stretch of Cys, Tyr side chain | G |
| | | 705 | COO ⁻ deform of amino acids | |
| | 730 | | C-S stretch of Cys | A |
| 760 | 773 | | indol sym. breath of Trp | |
| | 830 | 840 | Fermi resonance between ring breath and out-of-plane ring bend overtone of Tyr | |
| 895 | | 900 | C-C stretch of amino acids | |
| 930 | 945 | | C-C and C-COO ⁻ stretch of amino acids | |
| 980 | | | C-C stretch of proteins, CH in-plane bending of Phe | PO ₃ ²⁻ and C-O stretch |
| | 995 | 1005 | aromatic ring vib (e.g. of Phe) | |
| 1070/1089 | 1070/1089 | 1087 | NH ₂ rock, C-C and C-N stretch | PO ₂ sym stretch |
| | | | C-N and C-C stretch of proteins and lipids, NH ₃ ⁺ deform | |
| | 1120 | 1125 | | |
| 1145 | 1145 | 1150 | C-C stretch of Tyr, C-N stretch of proteins and lipids | |
| | 1170 | 1190 | CH ₃ rock of Thr | |
| 1210 | 1215 | | ring of Trp | |
| | | | Amide III, CH ₂ wag ring stretch, CH ₂ , CH ₃ deform of proteins | A, C |
| | | 1305 | | |
| | | 1335 | CH deform, CH ₂ and CH ₃ wag of proteins | |
| | | 1350 | CH ₂ sciss, CH ₃ deform of proteins, Trp | |
| | | 1465 | CH ₂ , CH ₃ deform, CH ₂ sciss of proteins and lipids | |
| 1530 | 1530 | | Amide II, N-H deform of proteins and lipids | |
| 1560 | 1555 | 1560 | Amide II of proteins, Trp | |
| 1590 | 1585 | | ring stretch, COO ⁻ asym. Stretch, Phe, Tyr | G, A |

Laser parameters in the LA-ICP-MS experiments

The ICP-MS Element XR (Thermo Fisher Scientific, *Germany*) was synchronized with the laser ablation unit (NWR213 from ESI, *USA*) in external triggering mode and daily tuned for maximum ion intensity and good signal stability (RSD < 5 %) using a glass slide. Helium was used as carrier gas and argon was added before reaching the ICP torch. The isotope ^{196}Pt was added to the method before ^{197}Au to ensure a stable magnetic field.

Table S2. NWR213 operating parameters.

| | |
|---|---------------|
| Wavelength / nm | 213 |
| Laser ablation method | Line scanning |
| He carrier gas flow rate/ L min ⁻¹ | 1.0 |
| Laser warm up / s | 30 |
| Wash out / s | 20 |
| Spot size / μm | 4 |
| Scan rate / $\mu\text{m s}^{-1}$ | 5 |
| Repetition rate / Hz | 10 |
| Fluence / J cm ⁻² | 0.7 |
| Line distance / μm | 6 |

Table S3. Element XR operating parameters.

| | |
|--|---|
| RF power / W | 1350 |
| Guard electrode | Platinum, active |
| Ar cooling gas flow rate / L min ⁻¹ | 15 |
| Ar auxiliary gas flow rate / L min ⁻¹ | 1.0 |
| Ar sample gas flow rate / L min ⁻¹ | 0.4 – 0.6 |
| Sample and skimmer cone | Ni |
| Mass resolution | Low (R = 300) |
| Scan optimization | Speed |
| Isotopes monitored | ^{197}Au (^{106}Pd , ^{107}Ag , ^{109}Ag , ^{196}Pt) |
| Magnet settling time / s | 0.1, 0.001, 0.001, 0.03, 0.001 |
| Runs x pass | 270-380 (depending on the length of the line) x 1 |
| Detection mode | All isotopes with SEM (triple) |
| Sample time / s | 0.002 |
| Samples per peak | 100 |
| Segment duration per isotope / s | 0.01 |
| Mass window per isotope / % | 5 |
| Search window / % | 0 |
| Integration window / % | 5 |
| Scan type | E-scan |

Table S4. iCAP Qc ICP-MS operating parameters used for solution analysis.

| | |
|--|--|
| Sample introduction system | Peltier-cooled cyclonic spray chamber (quartz glass) with MicroFlow PFA-ST nebulizer (100 $\mu\text{L min}^{-1}$) |
| RF power / W | 1550 |
| Ar cooling gas flow rate / L min^{-1} | 14 |
| Ar auxiliary gas flow rate / L min^{-1} | 0.8 |
| Ar sample gas flow rate / L min^{-1} | 1.1 |
| Sample and skimmer cone | Ni |
| Operation mode | Standard mode |
| Dwell time / ms | 100 |
| Main runs | 5 |
| Isotopes monitored | ^{197}Au , ^{175}Lu (internal standard) |

References

1. T. Büchner, D. Drescher, H. Traub, P. Schrade, S. Bachmann, N. Jakubowski and J. Kneipp, *Anal Bioanal Chem*, 2014, **406**, 7003-7014.
2. J. De Gelder, K. De Gussem, P. Vandenabeele and L. Moens, *J Raman Spectrosc*, 2007, **38**, 1133-1147.
3. A. Kudelski and W. Hill, *Langmuir*, 1999, **15**, 3162-3168.
4. F. S. Parker, *Applications of Infrared, Raman, and Resonance Raman Spectroscopy in Biochemistry*, Plenum Press: New York and London 1983.
5. S. Stewart and P. M. Fredericks, *Spectrochim Acta Part A Mol Biomol Spectrosc*, 1999, **55**, 1641-1660.
6. D. F. H. Wallach, *Chem Phys Lipids*, 1972, **8**, 347-354.
7. G. D. Fleming, J. J. Finnerty, M. Campos-Vallette, F. Celis, A. E. Aliaga, C. Fredes and R. Koch, *J Raman Spectrosc*, 2009, **40**, 632-638.
8. J. L. Lippert, L. E. Gorczyca and G. Meiklejohn, *Biochim Biophys Acta*, 1975, **382**, 51-57.
9. C. Otto, T. J. J. Vandentweel, F. F. M. Demul and J. Greve, *J Raman Spectrosc*, 1986, **17**, 289-298.